# Development and Balancing Control of a Unicycle Robot Using Omnidirectional Wheel

Phankon Pinkham and Manukid Parnichkun *

Industrial Systems Engineering, Engineering and Technology, Asian Institute of Technology, Pathum Thani, Thailand
Email: phankon30@gmail.com (P.P.); manukid@ait.ac.th (M.P.)
*Corresponding author

***Abstract*—A unicycle robot with an omnidirectional wheel mechanism is explained in this paper, focusing on its design and control. The proposed system combines a main driving wheel for pitch motion and a roller-based mechanism for lateral movement, allowing multi-directional movement while relying on single-wheel balance. A nonlinear dynamic model of the robot is derived using the Euler–Lagrange formulation and linearized around the upright equilibrium point to obtain a state-space representation. A Linear Quadratic Regulator (LQR) controller is designed to stabilize the roll and pitch motions simultaneously. Simulation results demonstrate fast stabilization with settling times of approximately 1.7 s for roll and 1.9 s for pitch. Experimental results on a unicycle robot confirm stable behavior with settling times of approximately 1.2 s and 1.5 s, respectively, and negligible steady-state error. The results support the effectiveness of mechanical design and control strategy for stable omnidirectional balancing.**

***Keywords*—unicycle robot, omnidirectional wheel, Linear Quadratic Regulator (LQR), self-balancing control, nonlinear dynamics**

## I. Introduction

Mobile robots are designed to minimize the contact points with the ground. This is a unique design approach that makes the robot highly agile. The unicycle robot illustrates this idea by relying on a single wheel and only one contact point to remain upright [1, 2]. This configuration reduces friction and allows for rapid directional changes, distinguishing it from multi-wheeled platforms [3]. As with other balancing robots, maintaining stability is a key challenge for the unicycle robot while performing movement work, requiring feedback control systems to guarantee balance [4, 5].#

Mobile robots have gained significant research attention due to their broad applications in fields like transportation, logistics, healthcare, and personal assistance [6, 7]. Recently, actuation, sensing, and control technologies have improved flexibility, speed, and precision in complex environments. Balancing robots present interesting challenges due to their need for simultaneous maneuver control and active stabilization [8]. Unicycle robots are a category of balancing robots that rely on a single wheel and are unstable, requiring feedback control methods to maintain balance during movement in any direction [9]. Reaction wheels, flywheels, or spherical wheels are often used in earlier designs to maintain balance, but these solutions often face problems from complex mechanisms and limited load capacity. While ball-balancing robots can move in any direction, they also face challenges in terms of dynamic modeling and mechanical limitations [10, 11].

Omnidirectional wheels allow robots to move in multiple directions, enabling robots to move in any planar direction without rotating themselves [12–14]. With Mecanum or omni-wheel designs, these wheels have been widely used in mobile robots, particularly in dynamic or confined environments. However, most omnidirectional configurations require multiple wheels, which limits their use in single-wheel robots. Recent research has explored integrating omnidirectional motion into unicycle robots using actuated wheel mechanisms. For example, the OmBURo robot uses an active omnidirectional wheel to enable planar motion while balancing on a single wheel [15]. Although it seems promising, these approaches reveal challenges in mechanical structure, actuation strategy, and dynamic modeling, highlighting the need for further exploration of alternative designs and control methods.

A unicycle robot is presented in this paper with a novel omnidirectional wheel mechanism. Unlike conventional designs with multiple or spherical wheels, the proposed system integrates a primary wheel for pitch motion and multiple roller wheels for lateral motion, all in a single wheel assembly. This configuration allows for omnidirectional wheel movement while maintaining a stable design for single-wheel balancing. The robot uses independent actuators for pitch and roll axes, with balance maintained through a suitable feedback control approach. A Linear Quadratic Regulator (LQR) controller is designed based on a dynamic model derived using the Euler–Lagrange formulation, and the system's nonlinear dynamics are linearized around the equilibrium point for controller design. The proposed control method is evaluated through both simulation and experiments on real hardware.

The main contribution of this study is the design and implementation of a timing-belt–synchronized

Manuscript received December 19, 2025; revised January 20, 2026; accepted March 23, 2026; published May 13, 2026.

omnidirectional wheel mechanism integrated into a single-wheel unicycle robot. The proposed transmission architecture combines spur gears, timing pulleys, and flexible shafts to coordinate roller motion within a compact wheel assembly, enabling stable omnidirectional movement while maintaining balance.#

## II. Literature Review

Unicycle balancing robots and omnidirectional mobile robots have received significant research attention due to their potential applications in mobile manipulation and personal transportation. Prior studies have investigated diverse balancing mechanisms, wheel designs, and control strategies to improve stability and maneuverability. While omnidirectional motion has been successfully achieved in multi-wheel platforms, its application to single-wheel balancing robots remains limited. The mechanical complexity of omnidirectional wheel integration and the coupled dynamics of unicycle robots pose significant challenges. This literature review summarizes existing work in these areas and identifies key limitations that motivate the design and control approach proposed in this paper.

### A. Single-Wheel and Unicycle Balancing Robots

Several control strategies have been proposed to address the inherently unstable and strongly coupled dynamics of single-wheel and unicycle robots. Model-based methods typically derive nonlinear dynamics using Newton–Euler, Lagrange, or Appell formulations, and then apply small-angle linearization to simplify controller design. Sliding Mode Control (SMC) has been used to decouple pitch, roll, and yaw subsystems, providing robustness against disturbances and parameter uncertainties [16]. Active Disturbance Rejection Control (ADRC) further improves robustness by using an extended state observer to estimate and compensate disturbances in real time, reducing dependence on an accurate model [17]. Reported simulations indicate that these approaches can stabilize the system with short settling times and maintain balance under external noise.

Adaptive and optimal control techniques have also been investigated to enhance performance. Dual-loop adaptive decoupling control based on neural PID structures allows online gain adjustment to handle nonlinearities and modeling errors [18]. For lateral (roll) stabilization, alternative mechanisms such as flywheel- or airflow-based actuators have been modeled and controlled using PID and LQR methods, where LQR generally achieves faster response and lower overshoot [19]. Overall, prior studies demonstrate effective stabilization of single-wheel platforms; however, achieving strong robustness, accurate decoupling, and reliable real-world performance under dynamic disturbances remains challenging.

### B. Omnidirectional Wheel Mechanisms

Omnidirectional wheel mechanisms have been widely investigated to overcome the nonholonomic constraints of conventional wheeled robots, enabling independent control of planar motion in $x-y$ translation and $yaw$ rotation. Among these mechanisms, Mecanum wheels are attractive due to their simple structure and their ability to generate lateral motion via angled passive rollers. Recent studies have extended Mecanum-based designs to dynamically balancing platforms. For instance, collinear Mecanum configurations have been integrated into wheeled inverted pendulum systems, achieving omnidirectional mobility while maintaining balance using a constrained dual-mode Model Predictive Control (MPC) framework that explicitly enforces torque and state constraints during multi-directional maneuvers [20]. Alternatively, paired Mecanum wheel units have been applied to two-parallel-wheel inverted pendulum platforms, where sagittal stabilization is combined with PID-based trajectory tracking and time-scaling strategies to reduce tracking deviation induced by balancing dynamics [21]. Although these studies confirm the feasibility of combining omnidirectional mechanisms with unstable self-balancing systems, challenges remain in coupling compensation, disturbance rejection, and high-accuracy tracking under dynamic motion, motivating further investigation in control design and system integration.

### C. Omnidirectional Unicycle Robots

Omnidirectional self-balancing robots have been widely explored through ballbot-type platforms, where three omnidirectional wheels are arranged 120° apart to actuate a single spherical wheel. In such systems, the robot behaves as a dual-axis inverted pendulum, and omnidirectional motion is achieved by controlling the ball's angular velocity in the $x$ and $y$ directions [22]. Although ball-driven designs enable smooth omnidirectional mobility with minimal footprint, their performance is highly dependent on friction conditions between the driving wheels and the ball. Slippage, surface contamination, and roller–ball contact inconsistencies may degrade tracking accuracy and disturbance rejection. Moreover, mechanical tolerances and vibration induced by roller discontinuities can introduce oscillations, which complicate stabilization and high-speed motion control [23].

To address these limitations, OmBURo introduces a novel unicycle robot equipped with an active omnidirectional wheel, in which both longitudinal motion and lateral motion are generated directly by actuated elements within a single wheel structure. Unlike passive Mecanum or ball-driven mechanisms, OmBURo employs a main driving wheel combined with actively driven peripheral rollers, enabling decoupled bidirectional control through two independent actuators [15]. This design reduces reliance on ground-ball friction and allows the robot to operate on inclined or uneven surfaces more robustly. However, the mechanical structure introduces new challenges: the transmission of torque to multiple rollers via gears and flexible shafts increases structural complexity, potential backlash, and friction losses. Maintaining synchronized roller motion while minimizing gaps between rollers is critical to avoid vibration and instability during balancing. Furthermore, the compact integration of dual actuators within a single wheel

constrains space, increases weight concentration, and may affect dynamic response. These trade-offs highlight that while active omnidirectional wheel mechanisms improve controllability and terrain adaptability, their mechanical design complexity and transmission losses remain key challenges for achieving high-efficiency, high-precision unicycle balancing systems.

### D. Control Strategies for Balancing Robots

In recent research, various control strategies have been applied to self-balancing robots to maintain stability and enable precise motion control. Among these strategies, Linear Quadratic Regulator (LQR) has emerged as a robust method, particularly for balancing unicycle robots and Wheel-Legged Robots (WLR). The LQR controller optimizes control inputs by minimizing a cost function, effectively stabilizing the robot's tilt and ensuring smooth motion, even on inclined surfaces [24]. For instance, in the unicycle robot, LQR controllers have been successfully used to maintain balance both on level ground and slopes, demonstrating excellent performance under varying tilt angles and conditions [25]. Similarly, the WLR platform, which combines wheeled and legged mechanisms, benefits from LQR-based balance control, enhancing its adaptability and stability across different terrains.

While LQR provides a powerful solution for balancing, other control strategies like Sliding Mode Control (SMC) and PID controllers have also been investigated for their robustness and simplicity. SMC, known for handling uncertainties and nonlinearities, is often used in two-wheeled balancing robots, decoupling balance and heading control, while offering robustness against external disturbances [26]. On the other hand, PID control is often employed in simpler systems for balancing and movement, where cascaded PID controllers manage both tilt and distance, allowing for smoother trajectory tracking [27]. However, compared to LQR, SMC and PID controllers face limitations in terms of tuning and handling complex disturbances. The integration of LQR with other controllers can offer an optimized solution for achieving high-efficiency, high-precision balance control across various robot types.

## III. Materials and Methods

The design, development, and experimental evaluation of the unicycle robot, including the accessories, the omnidirectional wheel mechanism, and the LQR controller, are described in this section. Fig. 1 shows the final 3D design of the unicycle balancing robot. The process is divided into hardware design, control system implementation, and experimental setup.

### A. Hardware Design

The unicycle robot is designed to apply a single omnidirectional wheel mechanism for omnidirectional motion while maintaining balance. Key components include:

#### 1) Omnidirectional wheel

The main wheel and roller wheels are combined for pitch motion and lateral movement. The robot is designed to move in any direction with minimal mechanical complexity. Fig. 2 shows the final 3D design of the wheel assembly and the defined pitch, roll, and yaw axes.

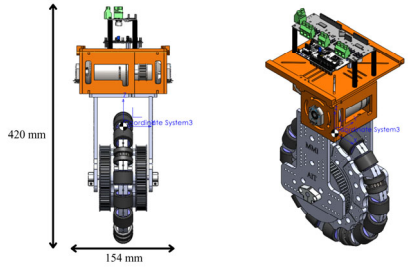


Fig. 1. The final 3D design of the unicycle balancing robot.

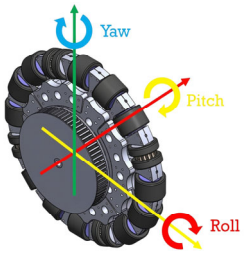


Fig. 2. The final 3D designs that show all of the wheel.

#### a) Pitch wheel design

The pitch wheel is designed to be the main actuator for the robot movement. It is mounted along the vertical axis of the robot, and it is directly responsible for adjusting the center of mass. This wheel is integrated with roller wheels that enable motion in any direction while allowing the robot to remain upright during dynamic motion. A DC motor drives the pitch wheel using encoder feedback for real-time position control, as illustrated in Fig. 3.

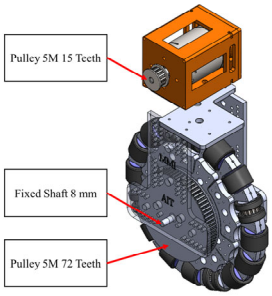


Fig. 3. Design of the drive system for the pitch axis.

#### b) Roller wheel design

The roller wheels are small rollers arranged around the pitch wheel, forming an integrated system that enables multi-directional motion. Each roller is installed at an angle to allow for both longitudinal and lateral movement. By using the rollers, the robot can move in any direction, including rotational motion, without additional steering mechanisms, which makes it good for moving in tight spaces.

The roller wheel system is driven by a spur gear inside the wheel assembly. A 32-tooth drive gear transmits torque to four 24-tooth spur gears, which are arranged to

distribute the load evenly across the mechanism. This configuration promotes smooth roller operation and enables omnidirectional motion. Using spur gears provides efficient torque transmission and helps improve the overall mechanical efficiency of the system. Fig. 4 illustrates the gear arrangement and the 32:24 gear ratio between the drive gear and the driven gears.

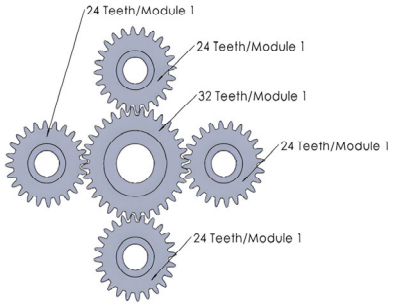


Fig. 4. Showing the ratio of all spur gears that is used inside the wheel.

To synchronize the roller motion and control the roll axis, a timing-belt pulley system is used. A 20-tooth timing pulley is mounted on the flexible shaft around the main wheel and serves as the driven pulley. The driving pulley is mounted on top of the spur-gear assembly and transmits torque to the 20-tooth pulley through the timing belt. This pulley coupling coordinates the motion of the small roller wheels for lateral movement and helps maintain a consistent orientation and stable motion on both flat and inclined surfaces. Fig. 5 displays the pulley system used to control the roll axis of the wheel. It shows how the pulleys are positioned and how they interact with the roller wheels.

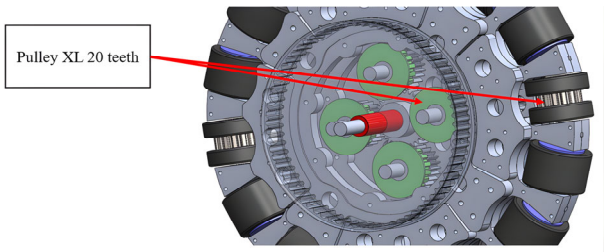


Fig. 5. The final 3D designs show the pulleys ratio of wheel to control the roll axis.

The roller wheel mechanism is central to the unicycle robot's omnidirectional movement. To enable this, the main wheel is designed with four sets of roller wheels, each set comprising three normal small roller wheels and one small roller wheel attached to a 20-tooth timing pulley. The timing pulley serves as the follower pulley, ensuring smooth transmission of motion to the roller wheels. All of the small pulleys are connected to flexible shafts, which allows for efficient power transmission and minimizes the loss of energy during operation. This configuration enables the robot to maintain omnidirectional movement while ensuring stability and maneuverability in a compact design, as shown in Fig. 6.

The flexible shafts used in the roller transmission mechanism are made of multi-layer wound spring steel, which is commonly used in mechanical power transmission systems that require both torque transmission and flexibility. This structure allows the shaft to transmit rotational torque from the driving pulley to the roller wheels while accommodating small bending angles inside the compact wheel assembly.

The helical multi-wire structure of the flexible shaft enables it to maintain torsional stiffness for torque transfer while allowing radial flexibility. This property allows the shaft to rotate continuously while bending along the wheel curvature, making it suitable for transmitting motion to multiple roller wheels arranged around the main wheel. As a result, the flexible shaft supports simultaneous rotational motion and bending deformation without significantly affecting torque transmission efficiency.

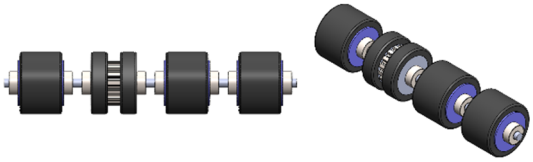

Fig. 6. The final 3D designs of rollers.

### *B. Electrical System Design*

The electrical system of the unicycle robot is designed for high efficiency and real-time processing, using an STM32 NUCLEO microcontroller as the central controller. This microcontroller processes all control algorithms, including the LQR controller, and communicates with external sensors and actuators. The robot's IMU sensor (BNO055) provides essential orientation data, including pitch, roll, and yaw, by combining accelerometer, gyroscope, and magnetometer functionalities. The BNO055 sensor communicates with the STM32 controller via the I2C interface, delivering real-time feedback crucial for maintaining stability. The robot's motion control is driven by BLDC motors controlled by an ODrive V3.6 motor driver. The motor driver adjusts the speed and torque to control the omnidirectional wheel's movement, ensuring smooth and precise operation.

For wireless communication, the ESP32 module enables Wi-Fi connectivity, allowing the robot to send and receive data remotely. This system enables real-time monitoring of the robot's performance, such as angle, speed, and torque values, directly to the user's computer. The STM32 NUCLEO processes this data and sends control signals to the ODrive V3.6 motor driver to regulate the motor speed and torque for balance and movement. The integration of these components ensures a robust and efficient system capable of executing omnidirectional movement and maintaining balance.

Fig. 7 shows the schematic diagram of the electrical system, illustrating how the STM32 NUCLEO board connects with the BNO055 IMU sensor via the I2C interface for real-time orientation data. The processed data from the IMU is used by the STM32 to compute control signals, which are then sent to the ODrive V3.6 motor driver using the USART interface. These signals control the BLDC motors, enabling the robot to perform precise movements while maintaining stability. The figure

provides a clear view of the data flow between the microcontroller, sensors, and actuators.

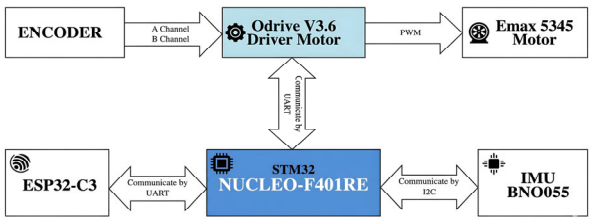


Fig. 7. Schematic diagrams of a circuit for the omnidirectional wheel robot.

## C. Mathematical Model of Unicycle Robot

The mathematical model of the unicycle robot is derived using the Euler–Lagrange method. This model describes the robot motion and is used for control design. It helps explain how the robot behaves, especially the relation between pitch, roll, and yaw motions. In this study, the robot is modeled as an inverted pendulum with two degrees of freedom: pitch and roll. The robot is driven by an omnidirectional wheel, which allows motion in different directions while keeping balance. Fig. 8 shows the real unicycle robot used for the model analysis. The robot includes sensors and actuators to measure motion and apply control based on the model.#

Fig. 8. The actual unicycle robot for analyzing.

Euler–Lagrange theory is used to derive the dynamic models of the unicycle robot. These dynamic models are crucial for controlling the robot, which is illustrated in Fig. 9. This figure represents the dynamic model of the robot, showing the forces and torques acting on the system.

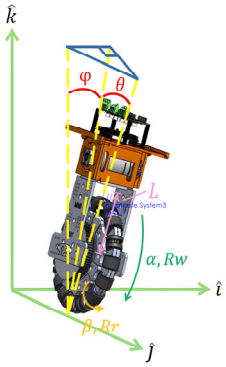


Fig. 9. The dynamic of unicycle robot.

#

### 1) Lagrangian formulation

The Lagrangian formulation starts by defining the rotational kinetic energy (T) and potential energy (V) of the unicycle robot. The Lagrangian (L) is then defined as# in Eq. (1):

$$L = T - V \tag{1}$$

### a) Rotational kinetic energy

The rotational kinetic energy of the unicycle robot is associated with the angular motion of the main wheel and the robot body. It depends on the moment of inertia and angular velocity of the rotating components. The rotational kinetic energy is expressed as in Eq. (2):

$$T = \frac{1}{2}[I_{by}a] + \frac{1}{2}[I_w b] + \frac{1}{2}[I_{bw}c] + \frac{1}{2}[I_{bx}d] \tag{2}$$

$$a = \left(\beta'^2 + \varphi'^2\right) \tag{3}$$

$$b = \alpha'^2 \tag{4}$$

$$c = \theta'^2 \tag{5}$$

$$d = \left(\theta'^2 + \alpha'^2\right) \tag{6}$$

where:

- $I_{by}$ is moment of inertia about body in roll axis.
- $I_{bx}$ is moment of inertia about body in pitch axis.
- $I_w$ is moment of inertia about wheel.
- $I_{bw}$ is inertia between body and wheel.

### b) Potential energy

The potential energy of the unicycle robot is mainly caused by gravity acting on the center of mass of the robot body. Since the robot behaves like an inverted pendulum, the potential energy depends on the vertical displacement of the center of mass with respect to the ground reference.

The gravitational potential energy is expressed as in Eq. (7):

$$V = M_{wh}\, gR_{wh}cos[\beta]cos[\alpha] + M_{bd}gL_{bd}cos[\theta]cos[\varphi] \tag{7}$$

where:

- $M_{wh}$ is mass of the wheel.
- $M_{bd}$ is mass of the body.
- $R_{wh}$ is the radius of the wheel.
- $L_{bd}$ is the length measured from the center of the wheel to the center of mass of the robot.
- $g$ is the gravitational acceleration.

### c) Equations of motion

The equations of motion for the unicycle robot are obtained by applying the Euler–Lagrange equation as in Eq. (8):

$$\frac{d}{dt}\left(\frac{\partial L}{\partial \dot{q}_i}\right) - \frac{\partial L}{\partial q_i} = \tau_i \tag{8}$$

where:

- $q_i$ is the generalized coordinates.
- $\tau_i$ is the generalized force acting on the system.

The generalized coordinates of the unicycle robot are selected as in Eq. (9):

$$q = [\varphi,\ \theta,\ \alpha,\ \beta] \tag{9}$$

where:

- $\varphi$ is the roll angle of the robot body.
- $\theta$ is the pitch angle of the robot body.
- $\alpha$ is the rotational angle of the main wheel.
- $\beta$ is the rotational angle of the roller mechanism.

The Euler–Lagrange equation is applied to each generalized coordinate as in Eqs. (10)–(13):

$$\varphi''[t] = -\frac{g cos[\theta]\ sin[\varphi]\ L_{bd} M_{bd} - 3.6 \times T_\beta}{I_{by}} \tag{10}$$

$$\theta''[t] = -\frac{g\ cos[\varphi]\ sin[\theta]\ L_{bd} M_{bd} - 4.8 \times T_\alpha}{I_{bx} + I_{bw}} \tag{11}$$

$$\beta''[t] = \frac{g\ cos[\alpha] sin[\beta]\ M_{wh} R_{wh} + T_\beta}{I_{by}} \tag{12}$$

$$\alpha''[t] = \frac{g\ cos[\beta]\ sin[\alpha]\ M_{wh} R_{wh} + T_\alpha}{I_{bx} + I_w} \tag{13}$$

where:

- $T_\theta$ is torque of robot in pitch axis.
- $T_\varphi$ is torque of robot in roll axis.
- $T_\alpha$ is torque of main wheel motor.
- $T_\beta$ is Torque of roller wheel motor.

The dynamic Eqs. (10)–(13) describe the nonlinear motion of the unicycle robot. The parameters used in the modeling process are defined based on the physical properties of the prototype system. These parameters are summarized in Table I.

TABLE I. PARAMETERS OF DYNAMIC MODEL

| Symbol | Description | Quantity | Unit |
|---|---|---|---|
| $I_w$ | Inertia of wheel | 0.013547 | Kg·m$^2$ |
| $I_{bw}$ | Inertia between body and wheel | 0.01993 | kg·m$^2$ |
| $I_{by}$ | Inertia of body in roll axis | 0.08052 | kg·m$^2$ |
| $I_{bx}$ | Inertia of body in pitch axis | 0.08646 | kg·m$^2$ |
| $M_{wh}$ | Mass of wheel | 3.073 | kg |
| $M_{bd}$ | Mass of body | 4.512 | kg |
| $R_{wh}$ | Radius of wheel | 0.1345 | m |
| $L_{bd}$ | The length measured from the center of the wheel to the center of mass of the robot. | 0.0916 | m |
| $g$ | Gravitational acceleration. | 9.8 | m/s$^2$ |

*2) State-space equation*

The nonlinear dynamic equations derived using the Euler–Lagrange formulation in Eqs. (10)–(13) represent a coupled second-order nonlinear system. Due to the presence of trigonometric nonlinearities and coupling between variables, direct controller design is complex. Therefore, the system is linearized around the upright equilibrium position. The equilibrium point is defined as in Eq. (14):

$$\varphi = 0,\ \theta = 0,\ \alpha = 0,\ \beta = 0 \tag{14}$$

which corresponds to the vertical balanced configuration of the robot.

Under the assumption of small angular deviations near the equilibrium point, the following small-angle approximations are applied:

$$sin(x) \approx x\ , cos(x) \approx 1 \tag{15}$$

where:

- $x$ belongs to the set $\{\varphi,\ \theta,\ \alpha,\ \beta\}$

After applying these approximations, the nonlinear dynamic equations are simplified into linear differential equations.

To express the system in state-space form, the second-order differential equations are converted into first-order form by defining the state vector as in Eq. (16):

$$x(t) = \left[\varphi\ \ \dot{\varphi}\ \ \theta\ \ \dot{\theta}\ \ \beta\ \ \dot{\beta}\ \ \alpha\ \ \dot{\alpha}\right]^T \tag{16}$$

where:

- $\dot{\varphi}$ is the roll angular velocity of the robot body.
- $\dot{\theta}$ is the pitch angular velocity of the robot body.
- $\dot{\beta}$ is the angular velocity of the roller mechanism.
- $\dot{\alpha}$ is the angular velocity of the main wheel.

The control input vector is defined as in Eq. (17):

$$u(t) = [T_\beta\ T_\alpha]^T \tag{17}$$

where:

- $T_\beta$ denote the motor torques applied to roller mechanisms.
- $T_\alpha$ denote the motor torques applied to the main wheel mechanisms.

The linearized dynamic model can then be expressed in standard state-space form as in Eq. (18)–(19):

$$\dot{x}(t) = Ax(t) + Bu(t) \tag{18}$$

$$y(t) = Cx(t) + Du(t) \tag{19}$$

where:

- $A$ is the system matrix.
- $B$ is the input matrix.
- $C$ and $D$ are the output matrices.

The system matrix $A$ and $B$ input matrix obtained from the linearized equations are given as follows:

$$A = \begin{bmatrix} 0 & 1 & 0 & 0 & 0 & 0 & 0 & 0 \\ \frac{gL_{bd}M_{bd}}{I_{by}} & 0 & 0 & 0 & 0 & 0 & 0 & 0 \\ 0 & 0 & 0 & 1 & 0 & 0 & 0 & 0 \\ 0 & 0 & \frac{gL_{bd}M_{bd}}{I_{bx}+I_{bw}} & 0 & 0 & 0 & 0 & 0 \\ 0 & 0 & 0 & 0 & 0 & 1 & 0 & 0 \\ 0 & 0 & 0 & 0 & \frac{gM_{wh}R_{wh}}{I_{by}} & 0 & 0 & 0 \\ 0 & 0 & 0 & 0 & 0 & 0 & 0 & 1 \\ 0 & 0 & 0 & 0 & 0 & 0 & \frac{gM_{wh}R_{wh}}{I_{bx}+I_w} & 0 \end{bmatrix} \tag{20}$$

$$B = \begin{bmatrix} 0 & 0 \\ -\frac{3.6}{I_{by}} & 0 \\ 0 & 0 \\ 0 & -\frac{4.8}{I_{bx}+I_{bw}} \\ 0 & 0 \\ \frac{1}{I_{by}} & 0 \\ 0 & 0 \\ 0 & \frac{1}{I_{bx}+I_w} \end{bmatrix} \quad (21)$$

$$C = \begin{bmatrix} 1 & 0 & 0 & 0 & 0 & 0 & 0 & 0 \\ 0 & 0 & 1 & 0 & 0 & 0 & 0 & 0 \\ 0 & 0 & 0 & 0 & 1 & 0 & 0 & 0 \\ 0 & 0 & 0 & 0 & 0 & 0 & 1 & 0 \end{bmatrix} \quad (22)$$

$$D = \begin{bmatrix} 0 & 0 \\ 0 & 0 \\ 0 & 0 \\ 0 & 0 \end{bmatrix} \quad (23)$$

*3) LQR controller*

After obtaining the linearized state-space representation in Eqs. (18) and (19), a Linear Quadratic Regulator (LQR) is designed to stabilize the unicycle robot around the upright equilibrium position.

The LQR method determines an optimal state-feedback control law of the form Eq. (24).

$$u(t) = -Kx(t) \quad (24)$$

where:

- $K$ is the optimal gain matrix.

The controller minimizes the quadratic cost function defined as in Eq. (25):

$$J = \int_0^\infty (x^T Q x + u^T R u)\, dt \quad (25)$$

where:

- $Q$ is the state weighting matrix.
- $R$ is the control weighting matrix.

In this study, the weighting matrices are selected as:

$$Q = \begin{bmatrix} 70 & 0 & 0 & 0 & 0 & 0 & 0 & 0 \\ 0 & 1 & 0 & 0 & 0 & 0 & 0 & 0 \\ 0 & 0 & 50 & 0 & 0 & 0 & 0 & 0 \\ 0 & 0 & 0 & 1 & 0 & 0 & 0 & 0 \\ 0 & 0 & 0 & 0 & 20 & 0 & 0 & 0 \\ 0 & 0 & 0 & 0 & 0 & 10 & 0 & 0 \\ 0 & 0 & 0 & 0 & 0 & 0 & 20 & 0 \\ 0 & 0 & 0 & 0 & 0 & 0 & 0 & 10 \end{bmatrix} \quad (26)$$

$$R = \begin{bmatrix} 100 & 0 \\ 0 & 100 \end{bmatrix} \quad (27)$$

Larger weights are assigned to the body angle states ($\varphi$ and $\theta$) to ensure rapid stabilization of the robot body, which is critical for maintaining balance. Moderate weights are assigned to wheel angle states, while smaller weights are given to angular velocity states to prevent excessive control effort. The weighting matrices were determined through iterative tuning in simulation to achieve a compromise between fast settling time, reduced overshoot, and actuator limitations.

The matrix $Q$ penalizes deviations of the state variables from the equilibrium, while $R$ penalizes excessive control effort.

The optimal gain matrix $K$ is obtained by solving the continuous-time Algebraic Riccati Equation (ARE) in Eq. (28):

$$A^T P + PA - PBR^{-1}B^T P + Q = 0 \quad (28)$$

where:

- $P$ is a positive-definite solution of the Riccati equation.

The feedback gain matrix is then computed as in Eq. (29):

$$K = R^{-1}B^T P \quad (29)$$

The resulting closed-loop system becomes Eq. (30).

$$\dot{x}(t) = (A - BK)x(t) \quad (30)$$

which ensures system stability if the pair A, B is controllable.

## IV. Results and Discussion

This section presents the results of both simulations and real-world experiments conducted to evaluate the performance of the unicycle robot equipped with an omnidirectional wheel and controlled by an LQR controller. The robot's performance was assessed in terms of roll and pitch angle control, settling time, overshoot, and energy efficiency.

### *A. Simulation Results*

The performance of the proposed LQR controller was first evaluated through MATLAB simulation using the linearized state-space model derived in Section III. The simulation was conducted to verify system stability and dynamic response under initial disturbances.

*1) Roll angle response*

The simulated roll angle response of the unicycle robot under LQR control is shown in Fig. 10. An initial disturbance was applied in the roll direction to evaluate the stabilization capability of the controller.

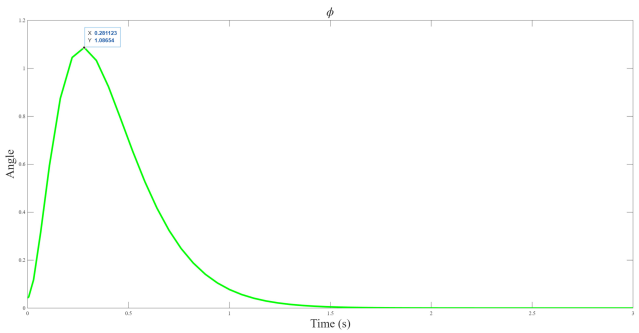


Fig. 10. The simulation result of roll angle.

As observed in Fig. 10, the roll angle increases to a peak transient value of approximately 1.08° before smoothly converging toward the equilibrium position. The response does not exhibit sustained oscillations, indicating that the closed-loop system is well damped.

The roll angle settles within approximately 1.7 s, and the steady-state error is negligible. These results demonstrate that the proposed LQR controller effectively stabilizes the robot in the roll direction and rapidly suppresses angular deviations.

*2) Pitch angle response*

The simulated pitch angle response of the unicycle robot under LQR control is shown in Fig. 11. An initial disturbance was applied in the pitch direction to evaluate the stabilization performance of the proposed controller.

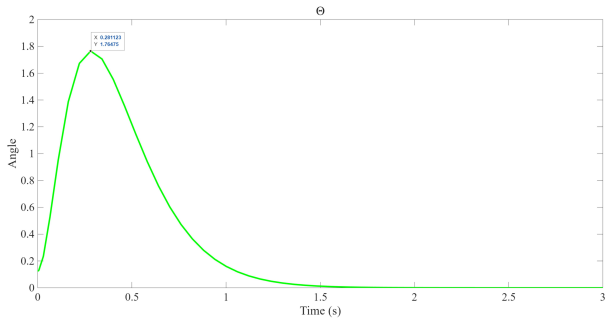


Fig. 11. The simulation result of pitch angle.

As observed in Fig. 11, the pitch angle reaches a peak transient value of approximately 1.76° before smoothly converging toward the equilibrium position. The response exhibits no sustained oscillation, indicating a well-damped closed-loop system.

The pitch angle settles within approximately 1.9 s, and the steady-state error is negligible. These results confirm that the LQR controller effectively stabilizes the robot in the pitch direction while maintaining stable dynamic behavior.

## B. Experimental Results

To validate the effectiveness of the proposed LQR controller under real operating conditions, the control algorithm was implemented on the physical prototype of the unicycle robot. The experiments were conducted on a flat surface with the robot initially disturbed from its equilibrium position, as shown in Fig. 12.

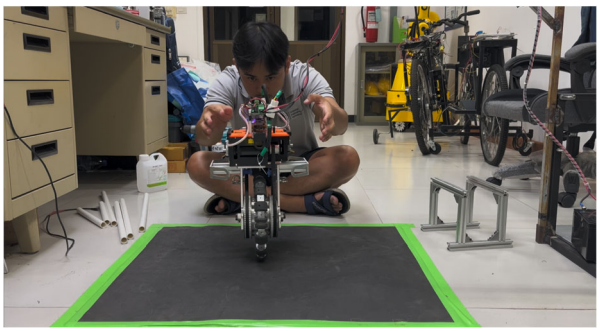

Fig. 12. Experimental setup of the unicycle robot.

*1) Experimental roll angle response*

The actual experimental roll angle response of the unicycle robot under LQR control is shown in Fig. 13. The robot was subjected to an external disturbance in the roll direction to evaluate real-world stabilization performance.

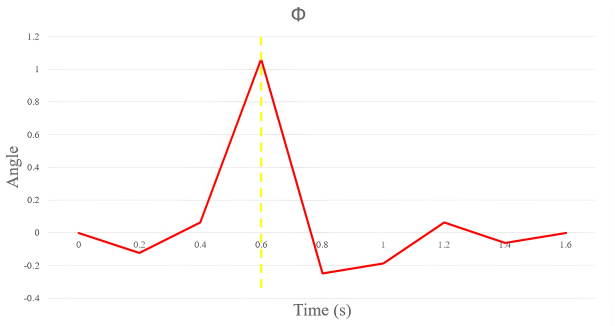


Fig. 13. Experimental roll angle response under LQR control.

As observed in Fig. 13, the roll angle reaches a peak deviation of approximately 1.1° at around 0.6 s before rapidly converging toward the equilibrium position. After the transient response, the system exhibits small fluctuations due to sensor noise and mechanical vibration.

The roll angle settles within approximately 1.2 s, and the steady-state error remains close to zero. These results confirm that the proposed LQR controller effectively stabilizes the robot under practical operating conditions.

*2) Experimental pitch angle response*

The experimental pitch angle response under LQR control is shown in Fig. 14. An external disturbance was applied to evaluate the real-world stabilization performance of the robot in the pitch direction.

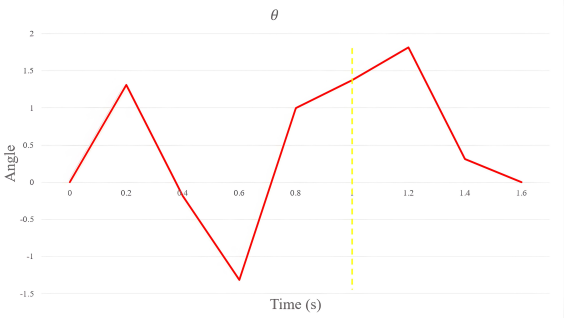


Fig. 14. Experimental pitch angle response under LQR control.

As observed in Fig. 14, the pitch angle exhibits a transient oscillatory response with a maximum positive deviation of approximately 1.8° and a minimum negative deviation of approximately −1.4°. The oscillations gradually decrease, and the system converges toward the equilibrium position.

The pitch angle settles within approximately 1.5 s, and the steady-state error is negligible. The slight oscillations observed in the response are mainly attributed to sensor noise, mechanical vibration, and unmodeled nonlinearities in the physical system.

### C. Quantitative Performance Comparison

To quantitatively evaluate the effectiveness of the proposed LQR controller, a comparison between simulation and experimental results is summarized in Table II. The key performance metrics include settling time, peak angle deviation, and steady-state error for both roll and pitch motions.

The larger peak angle observed in simulation corresponds to the imposed initial disturbance used for robustness evaluation, whereas the experimental disturbance magnitude was intentionally smaller for safety considerations.

TABLE II. COMPARISON BETWEEN SIMULATION AND EXPERIMENTAL RESULTS

| Performance Metric | Simulation | Experiment |
|---|---|---|
| Roll Settling Time | 1.7 s | 1.2 s |
| Pitch Settling Time | 1.9 s | 1.5 s |
| Peak Roll Angle | 1.08° | 1.1° |
| Peak Pitch Angle | 1.76° | 1.8° |
| Steady-State Error | ~0° | ~0° |

The experimental results show slightly slower convergence compared to simulation due to unmodeled friction, actuator dynamics, sensor noise, and hardware nonlinearities. However, the overall behavior is consistent, validating the accuracy of the derived model and the effectiveness of the LQR controller.

## V. CONCLUSION

This paper presented the design and control of a unicycle robot equipped with an omnidirectional wheel mechanism. A nonlinear dynamic model was derived using the Euler–Lagrange formulation and linearized around the upright equilibrium point to obtain a state-space representation suitable for controller design. An LQR controller was implemented to stabilize both roll and pitch motions simultaneously.

Simulation results demonstrated fast and stable convergence, with settling times of approximately 1.7 s for roll and 1.9 s for pitch. Experimental validation on the physical prototype confirmed stable behavior under real operating conditions, achieving settling times of approximately 1.2 s and 1.5 s with negligible steady-state error. The experimental results closely matched the simulation predictions, validating the accuracy of the proposed model and the effectiveness of the control strategy.

Overall, the proposed mechanical design and LQR-based control approach provide a feasible solution for achieving stable omnidirectional motion in a single-wheel balancing robot. Future work may focus on improving disturbance rejection performance and extending the system for trajectory tracking and autonomous navigation.

## CONFLICT OF INTEREST

The authors declare no conflict of interest.

## AUTHOR CONTRIBUTIONS

Phankon Pinkham was responsible for methodology, software development, experimentation, and manuscript writing. Prof. Manukid Parnichkun contributed to supervision, conceptualization, and manuscript review. All authors have read and approved the final manuscript.

## REFERENCES


[1] M.-T. Ho, Y. Rizal, and Y.-L. Chen, "Balance control of a unicycle robot," in *Proc. IEEE 23rd Int. Symp. Ind. Electron. (ISIE)*, Istanbul, Turkey, 2014, pp. 1186–1191. doi: 10.1109/ISIE.2014.6864782

[2] K. S. Thar, D. Maneetham, M. M. Aung, and T. Rabgyal, "Design and development of the unicycle balancing robot using linear slider," in *Proc. 11th Int. Conf. Cyber IT Service Management (CITSM)*, Makassar, Indonesia, 2023, pp. 1–6. doi: 10.1109/CITSM60085.2023.10455243

[3] M. A. Rosyidi, E. H. Binugroho, S. E. R. Charel, R. S. Dewanto, and D. Pramadihanto, "Speed and balancing control for unicycle robot," in *Proc. Int. Electron. Symp. (IES)*, Denpasar, Indonesia, 2016, pp. 19–24. doi: 10.1109/ELECSYM.2016.7860969

[4] G. Daoxiong and L. Xiang, "Yaw control for a self-balancing unicycle robot with two flywheels," in *Proc. 32nd Chin. Control Conf. (CCC)*, Xi'an, China, 2013, pp. 5576–5582.

[5] P. Wang, Q. Lu, X. Zhao, and H. Zhang, "Finite-time posture control of a unicycle robot," in *Proc. 34th Chin. Control Conf. (CCC)*, Hangzhou, China, 2015, pp. 1151–1156. doi: 10.1109/ChiCC.2015.7259796

[6] Y. Liu, Y. Li, L. Shi, and Z. Lin, "Leader-following formation control for cooperative transportation of multiple mecanum-wheeled mobile robots," *IEEE Trans. Intell. Transp. Syst.*, 2026. doi: 10.1109/TITS.2026.3652216

[7] B. Paro, J. Rogina, L. Petrović, M. Seder, and I. Marković, "Coordinated planning and control of two mobile robots for joint cargo transportation," in *Proc. 11th Int. Conf. Autom. Robot. Appl. (ICARA)*, Zagreb, Croatia, 2025, pp. 200–204. doi: 10.1109/ICARA64554.2025.10977646

[8] S. Basovich, S. Arogeti, Z. Brand, and N. Levi, "Nonlinear control of a novel active magnetic bearings technology based high-precision positioning stage," in *Proc. 21st Mediterr. Conf. Control Autom. (MED)*, Platanias, Greece, 2013, pp. 1464–1469. doi: 10.1109/MED.2013.6608914

[9] H. Zhang and N. Mohamad Nor, "Control strategies for two-wheeled self-balancing robotic systems: A comprehensive review," *Robotics*, vol. 14, no. 8, 101, 2025. doi: 10.3390/robotics14080101

[10] D. N. Nguyen, T. B. Cao, T. H. Pham, N. T. Vo, P. V. Dang, and H. N. Le, "Design and control of a ball-balancing robot," in *Proc. 4th Int. Conf. Green Technol. Sustain. Develop. (GTSD)*, Ho Chi Minh City, Vietnam, 2018, pp. 317–322. doi: 10.1109/GTSD.2018.8595602

[11] A. Hasan, "Exogenous Kalman filter for state estimation in autonomous ball balancing robots," in *Proc. IEEE/ASME Int. Conf. Adv. Intell. Mechatronics (AIM)*, Boston, MA, USA, 2020, pp. 1522–1527. doi: 10.1109/AIM43001.2020.9158896

[12] R. Cao, J. Gu, C. Yu, and A. Rosendo, "Omniwheg: An omnidirectional wheel-leg transformable robot," in *Proc. IEEE/RSJ Int. Conf. Intell. Robots Syst. (IROS)*, Kyoto, Japan, 2022, pp. 5626–5631. doi: 10.1109/IROS47612.2022.9982030

[13] W.-H. Tung, H.-M. Wu, and Y.-F. Lin, "Sensor fusion based obstacle avoidance and path following for a mecanum wheel omnidirectional robot," in *Proc. 25th Int. Conf. Control Autom. Syst. (ICCAS)*, Incheon, Republic of Korea, 2025, pp. 989–994. doi: 10.23919/ICCAS66577.2025.11301267

[14] F. Iotti, A. Ranjan, F. Angelini, and M. Garabini, "Omniquad: A wheeled-legged hybrid robot with omnidirectional wheels," *Mech. Mach. Theory*, vol. 214, Art. no. 106125, 2025. doi: 10.1016/j.mechmachtheory.2025.106125

[15] J. Shen and D. Hong, "Omburo: A novel unicycle robot with active omnidirectional wheel," in *Proc. IEEE Int. Conf. Robot. Autom. (ICRA)*, Paris, France, 2020, pp. 8237–8243. doi: 10.1109/ICRA40945.2020.9196927

[16] L. Guo, K. He, and Y. Song, "Design of the sliding mode controller for a kind of unicycle robot," in *Proc. IEEE Int. Conf. Inf. Autom. (ICIA)*, Ningbo, China, 2016, pp. 1432–1437. doi: 10.1109/ICInfA.2016.7832044

[17] X. Ruan, X. Wang, X. Zhu, Z. Chen, and R. Sun, "Active disturbance rejection control of single wheel robot," in *Proc. 11th World Congr. Intell. Control Autom. (WCICA)*, Shenyang, China, 2014, pp. 4105–4110. doi: 10.1109/WCICA.2014.7053403

[18] X. Ruan, Q. Wang, and N. Yu, "Dual-loop adaptive decoupling control for single wheeled robot: Based on neural PID controller," in *Proc. 11th Int. Conf. Control Autom. Robot. Vision (ICARCV)*, Singapore, 2010, pp. 2349–2354. doi: 10.1109/ICARCV.2010.5707433

[19] X. Ruan and W. Xie, "Lateral dynamic modelling and control of a single wheel robot based on airflow flywheel," in *Proc. IEEE Int. Conf. Mechatronics Autom. (ICMA)*, Beijing, China, 2015, pp. 2192–2196. doi: 10.1109/ICMA.2015.7237826

[20] M. T. Watson, D. T. Gladwin, T. J. Prescott, and S. O. Conran, "Dual-mode model predictive control of an omnidirectional wheeled inverted pendulum," *IEEE/ASME Trans. Mechatronics*, vol. 24, no. 6, pp. 2964–2975, 2019. doi: 10.1109/TMECH.2019.2943708

[21] S. Miyakoshi, "Omnidirectional two-parallel-wheel-type inverted pendulum mobile platform using mecanum wheels," in *Proc. IEEE Int. Conf. Adv. Intell. Mechatronics (AIM)*, Munich, Germany, 2017, pp. 1291–1297. doi: 10.1109/AIM.2017.8014196

[22] M. Kumagai and T. Ochiai, "Development of a robot balancing on a ball," in *Proc. Int. Conf. Control Autom. Syst. (ICCAS)*, Seoul, Republic of Korea, 2008, pp. 433–438. doi: 10.1109/ICCAS.2008.4694680

[23] H. Y. Han, T. Y. Han, and H. S. Jo, "Development of omnidirectional self-balancing robot," in *Proc. IEEE Int. Symp. Robot. Manuf. Autom. (ROMA)*, Kuala Lumpur, Malaysia, 2014, pp. 57–62. doi: 10.1109/ROMA.2014.7295862

[24] D. Gong, Q. Pan, G. Zuo, and W. Deng, "LQR control for a self-balancing unicycle robot," in *Proc. 10th World Congr. Intell. Control Autom. (WCICA)*, Beijing, China, 2012, pp. 1424–1429. doi: 10.1109/WCICA.2012.6358103

[25] J. Dong, R. Liu, B. Lu, X. Guo, and H. Liu, "LQR-based balance control of two-wheeled legged robot," in *Proc. 41st Chin. Control Conf. (CCC)*, Hefei, China, 2022, pp. 450–455. doi: 10.23919/CCC55666.2022.9902200

[26] N. Hasanah, S. A. Rahmah, W. P. Sari, N. Tamami, Alrijadjis, and B. Sumantri, "Movement control of two wheels balancing robot using SMC based on Lyapunov analysis," in *Proc. 2nd Int. Conf. Appl. Inf. Technol. Innov. (ICAITI)*, Denpasar, Indonesia, 2019, pp. 37–43. doi: 10.1109/ICAITI48442.2019.8982121

[27] D. Pratama, E. H. Binugroho, and F. Ardilla, "Movement control of two wheels balancing robot using cascaded PID controller," in *Proc. Int. Electron. Symp. (IES)*, Surabaya, Indonesia, 2015, pp. 94–99. doi: 10.1109/ELECSYM.2015.7380821

Copyright © 2026 by the authors. This is an open access article distributed under the Creative Commons Attribution License which permits unrestricted use, distribution, and reproduction in any medium, provided the original work is properly cited (CC BY 4.0)